International Journal of Engineering Research & Technology (IJERT)
ISSN: 2278-0181
Vol. 11 Issue 09, September 2022

Evaluation of Defluoridation of Water by Adsorption with Sugarcane Bagasse derived Activated Carbon

Ian Mwenda Mugambi, Peter Kuria Ndiba, Zabloo Oonge
Civil & Construction Engineering
University of Nairobi
Nairobi, Kenya

Abstract **- Sustained consumption of water with fluoride concentrations above the WHO guideline value of 1.5 mg/L is of health concern because of its contribution to dental and skeletal fluorosis, and neurological and thyroid disorders. Accordingly, the development of a cost-effective, locally available and environmentally benign adsorbent for fluoride removal from water is of importance. In the present study, oven dried and ground sugarcane bagasse was calcined at 500°C for 2 hours and then activated with 30% aqueous solution of phosphoric acid. The resulting sugarcane bagasse derived activated carbon (SBAC) was characterized by proximate analysis, ultimate analysis, nitrogen adsorption, scanning electron microscopy, FT-IR spectroscopy, and X-ray diffraction. The potential for fluoride removal from water with SBAC was evaluated for adsorbent dosage, contact time, pH and initial fluoride concentration. Calcination and activation increased fixed carbon concentration from 19.1 to 69.7%. Pore volume and BET surface area measurement showed that micropores accounted for 84% of the total pore volume. The FTIR spectrum revealed the presence of surface functional groups including C=C, P–O-C and P–O–P, which could play a significant role in the SBAC sorption of fluoride. The SBAC applied at 20 g/250 ml of water, 5 h contact time and pH 5 reduced the fluoride concentration in fluoride simulated water by 86% from 7.0 to 0.98 mg/L. A lesser removal of 82.7% was observed for natural groundwater with 6.7 mg/l fluoride concentration and was attributed to competition for active sites by coexisting ions. The Langmuir isotherm did not adequately describe the adsorption data suggesting a lack of uniformity on the adsorption surface.**

Keywords—Activated Carbon; Defluoridation; Fluoride; Sugarcane Bagasse; Micropores;

I. INTRODUCTION

Fluoride is present in groundwater, mainly from natural processes such as rock erosion and volcanic activity but also from effluent of industries such as fertilizer manufacturing and electroplating works [1]. Fluoride ion in drinking water can have positive or negative effects on human health depending on its concentration [2]. The ion is a micronutrient for the human body, which helps in prevention of tooth decay by decreasing the rate of removal of essential minerals in teeth [3]. However, sustained consumption of water with fluoride concentrations greater than 1.5 mg L^{-1} may lead to irreversible skeletal and dental fluorosis, the demineralization of bones and tooth tissues [4]. Fluoride related health complications have been observed along the Rift Valley of Kenya with fluoride concentrations of up to 7.69 mg L^{-1} [5].

Fluoride concentration in groundwater varies widely with geographic location. Areas with high fluoride concentration tend to coincide with volcanic rocks in and around the Rift Valley Region of Kenya. Elevated concentrations of fluorides were found in areas which have fluorspar deposits such as Nakuru Town, Gilgil, Elementaita and Koibatek-Baringo. The highest natural fluoride concentration ever recorded in natural water was 2,800 mg L^{-1} in Lake Nakuru [6].

Available defluoridation techniques include precipitation/coagulation, adsorption methods, reverse osmosis, ion-exchange and electro-dialysis. Most of these techniques require skilled labour to operate and have large capital and operational costs, which make them technically and financially non-feasible for less developed communities [7]. For example, reverse osmosis processes and ion exchange are rarely used in developing countries because of their large initial and operational costs. Electro-dialysis processes that transfer fluoride ions through a semi-permeable membrane as a result of electric potential gradient also have high initial capital cost and are easily affected by coexisting ions [7]. Therefore, there is a need to search for alternative fluoride removal techniques that are simple to use and affordable to less developed communities [8].

The removal of fluoride from water with activated carbon takes place through several mechanisms, largely adsorption. The efficiency of the defluoridation depends on the characteristics of the activated carbon [9]. Activated carbon derived from agricultural by-products has been found to be relatively inexpensive largely because of the availability of by-products of agricultural processing in substantial quantities. Sugarcane bagasse, a waste product of sugarcane processing, is produced in large quantities, which often poses challenges of disposal. Consequently, the use of bagasse for production of activated carbon could also assist in reduction of the volume of the bagasse that requires disposal [10]. This study evaluated the use of sugarcane bagasse derived activated carbon (SBAC) in defluoridation of laboratory simulated fluoride water and natural groundwater with elevated fluoride concentration.

II. MATERIALS AND METHODS

A. Preparation of Activated Carbon

Sugarcane bagasse was obtained from sugarcane juice venders in Nairobi and rinsed severally with tap water followed by hot distilled water to wash out foreign substances. The washed bagasse was dried at room temperature of 20°C, for 3 days. It was then chopped to small pieces of less than 3 mm size and dried in an oven at 110°C for 24 hours. After drying, the bagasse was ground with mortar and pestle and sieved. The ground bagasse was carbonized by heating in a box-type

International Journal of Engineering Research & Technology (IJERT)
ISSN: 2278-0181
Vol. 11 Issue 09, September 2022

resistance furnace at 500°C for 2 hours. The produced carbon was activated with 30% aqueous solution of phosphoric acid (H_3PO_4) at a weight ratio of 1:1 for 24 hours. The activated carbon was washed with triple-distilled water several times to achieve an effluent pH of 7. It was then oven dried at 110°C for 2 hours [11]. Finally, the activated carbon was passed through a 0.5 mm sieve and stored in a sealed polyethylene bag for characterization and use in adsorption tests [12].

B. Characterization of Ground Raw Sugarcane Bagasse and SBAC

Raw ground sugarcane bagasse and SBAC were characterized for proximate and ultimate composition, surface area, functional groups, surface profile, crystallinity, and distribution of micropores and mesopores and bulk density. To further assist in evaluation of product preparation, the yield of activated carbon from sugarcane bagasse was determined.

C. Proximate and Ultimate Analysis

The proximate analysis for moisture, volatile content, fixed carbon and ash contents followed ASTM D7582-10. The ultimate analysis to determine carbon, oxygen, hydrogen, and nitrogen contents of the samples was carried out with CHNS-O Analyzer model FlashEA, 1112 Series [13].

D. Surface Area Analysis

The specific surface area, pore volume, and pore size distribution of the sugarcane bagasse activated carbon were determined from the adsorption isotherms with Brunauer–Emmett–Teller (BET) equation and Quantachrome Nova Win2© 1994– 2002 instrument. The cross-sectional area of a nitrogen molecule was assumed as 0.162 nm. The Dubinin–Radushkevich (DR) equation was used to compute the volume of micropores. The total pore volume was estimated to be the liquid volume of the adsorbate (N_2) at a relative pressure of 0.985. The pore size distribution was determined with the BJH model. The average pore diameter was calculated as 4 times the total pore volume over the BET surface area [14].

E. Scanning Electron Microscopy (SEM)

SBAC was scanned with a Leica Cambridge S-360 scanning electron microscope (SEM). The samples were placed onto a SEM holder with double-sided electrically-conducting carbon adhesive tabs to prevent the surface of the specimens when exposed to the electron beam. The samples were coated with a 20 nm thick layer of gold with a Polaron Equipment Limited model E500, set at a voltage of 1.2 kV (10 mA) and a vacuum 20 Pa for 10 min.

F. Fourier Transform Infra-Red (FT-IR) Analysis of functional group

An FT-IR spectrophotometer was used to detect different functional groups in the activated carbon. The spectrophotometer used a Nicolet Avatar Model 360 instrument with potassium bromide (KBr) pellets for wavelengths ranging from 4000 to 400 cm^{-1}. Spectra were obtained with dried powdered samples recorded as KBr disks on a Nicolet AVATAR 360 Fourier Transform Infrared Spectrophotometer. Approximately 1 mg samples were mixed in a matrix of KBr (100 mg) and pressed to form test pellets [13].

G. X-Ray Diffraction Analysis (XRD)

X-ray diffraction analysis was conducted on SBAC to determine its crystallinity or amorphous nature. Analyses were performed by Philips PW1050 X-pert diffractometer with Cu-K (= 0.15406 Å) radiation source operating under a voltage of 40 kV and a current of 25 mA. The diffraction angle (2) was varied from 2.5 to 10. Activated carbons were analyzed for their orientation within the matrix material. The diffractograms were analyzed by X-pert Highscore Plus Software. The X-ray diffraction patterns were collected with a scan rate of 4.2 C/min.

The degree of crystallinity was calculated from the area of crystalline peaks of diffraction A_C and the area of amorphous peaks of diffraction A_a from Eq. (1).

$$X_c = \frac{A_c}{(A_c + A_a)} \quad (1)$$

where, X_c is the degree of crystallinity, A_c is the crystallized area on the X-ray diffractogram, A_a is the amorphous area on the X-ray diffractogram.

H. Bulk Density

A measuring cylinder 200 ml was first adjusted to zero on the weighing balance. The activated carbon with running consistency was then taken and poured into the measuring cylinder to the 200 ml mark tapping the cylinder to ensure no void was created. The weight was recorded and the bulk density calculated.

I. Distribution of Mesopores and Micropores

The distribution of mesopores was analyzed by the Barrett–Joyner–Halenda method, while that of micropores was analyzed by the t-plot and Horvath–Kawazoe methods.

J. Activated Carbon Yield

Activated Carbon yield was computed as the weight of final activated carbon produced after activation, sorting, and washing divided by the mass of the original raw materials on a dry basis as shown in Eq. (2)

$$\text{Yield } (\%) = \frac{w_c}{w_o} \text{ x } 100\% \quad (2)$$

where w_c is the weight of activated carbon (g) and w_o is the weight of dry precursor (g).

K. Fluoride Analysis and Fluoride Adsorption Tests

Stock solution of laboratory simulated fluoride water with 100 mg/L concentration was prepared by dissolving 0.221 mg of sodium fluoride (NaF) in 1 L of triple distilled water. Natural fluoridated water samples were collected from an operating borehole in Nakuru Town, coordinates 0°10'50" S, 35° 59' 28" E. The sampling was carried at peak water usage at midday for 20 minutes to purge the system before collection of test samples. The samples were collected in three 20 litres plastic sampling containers pre-rinsed with distilled water and tightly capped and transported in cooling boxes to University of Nairobi's Environmental Engineering Laboratory for analysis and the adsorption tests.

All batch experiments were conducted with 250 mL of aqueous solution containing known fluoride concentration in flasks to which a weighed amount of SBAC was added. The flask contents were stirred continuously at room temperature to achieve equilibrium. Samples were drawn from each flask at intervals and filtered through a Whatman No. 42 filter paper

International Journal of Engineering Research & Technology (IJERT)
ISSN: 2278-0181
Vol. 11 Issue 09, September 2022

before fluoride analysis. All the adsorption tests were performed in triplicate. The adsorption removal efficiency and the defluoridation capacity (mg F- adsorbed/g of adsorbent) at a given contact time for the selected adsorbents were determined with the Eqs. (3) and (4) [15], [16].

$$\text{Percentage removal} = \frac{(C_O - C_t)}{C_o} \times 100 \quad (3)$$

$$\text{Adsorption capacity} = \frac{(C_O - C_t)}{m} \times V \quad (4)$$

where, C_0 is initial fluoride concentration in mg/L, C_t is residual fluoride concentration in mg/L at time t, m is mass of the adsorbent in g, and V is volume in L of the solution used in the batch tests.

III. Evaluation of Effects of Adsorption Parameters on Removal of Fluoride

A. *Effect of Adsorbent Dosage and Contact Time*

Adsorbent tests were performed for dosages of 5, 10, 15, 20 and 25 g in 250 ml of fluoride water with initial fluoride concentration 7.0 mg/L and pH 6.5. The samples were collected at intervals of 30 minutes for 5 hours.

B. *Effect of pH*

The influence of solution pH on defluoridation tests were conducted on test solutions containing 7.0 mg/L of fluoride adjusted to pH values of 3, 4, 5, 6, 7, 8, 9 and 10 with 1 N HCl and 1 N NaOH.

C. *Effect of Initial Fluoride Concentration*

The effects of initial fluoride concentration tests were conducted at fluoride concentrations of 5, 10, 15, 20 mg/L at selected conditions: 20 g SBAC /250 ml dosage, 5 h contact time, pH 3.

D. *Groundwater Defluoridation Tests*

Samples of groundwater with elevated concentrations of fluoride were collected from Nakuru, Kenya in 5-L plastic bottles cleaned with deionized water. The fluoride removal efficiency from the natural water samples by SBAC was tested under the selected conditions: 20 g SBAC /250 ml dosage, 5 h contact time, pH 3.

E. *Experiments for Adsorption Isotherms*

Adsorption isotherms are useful models for the description of adsorption processes by different adsorbents. The Langmuir model assumes uniform adsorption energies on the adsorbent surface and no transmigration of the adsorbate in the plane of the surface. On the other hand, the Freundlich model can describe adsorption by heterogeneous surfaces.

Adsorption tests for isotherms were conducted at constant SBAC dosage of 100 mg in 250 ml of fluoride water over initial fluoride concentrations 5, 10, 20, 50, 75 and 100 mg/ 250 ml at pH 3. The mixture was agitated for 24 h to achieve equilibrium and then filtered through a Whatman No. 42 filter paper. The mass of fluorides adsorbed per mass of the adsorbent, q_e, was computed from Eq. (5)

$$q_e = \frac{(C_o - C_e)V}{m} \quad (5)$$

where V is the volume of the water sample in L, C_o and C_e were the initial and equilibrium fluoride concentration in mg/L, and m is the mass in g of the adsorbent.

The experimental data was fitted into a linearized form of the general Langmuir isotherm as expressed in Eq. (6)

$$\frac{C_e}{q_e} = \frac{1}{bq_0} + \frac{1}{q_0} C_e \quad (6)$$

where Ce equilibrium is the concentration in mg/L, q_o maximum adsorption capacity for a monolayer in mg/g, q_e absorptivity capacity at equilibrium in mg/g, and b Langmuir isotherm constant in L/ mg [17].

The essential characteristics of Langmuir isotherm can be expressed in terms of a dimensionless constant, separation factor or equilibrium parameter R_L as defined by Eq. (7)

$$R_L = \frac{1}{1+bC_0} \quad (7)$$

where C_o is the initial fluoride concentration in mg/L; and b is the Langmuir constant in L/mg.

The R_L value indicates the type of isotherm to be irreversible ($R_L = 0$), favourable ($0<R_L<1$), linear ($R_L = 1$), and unfavourable ($R_L>1$) [18].

The data was also fitted into the Freundlich Isotherm expressed in Eq. (8) by plotting $\log(q_e)$ against $\log(C_e)$.

$$q_e = k_f C_e^{\frac{1}{n}} \quad (8)$$

where the q_e (mg/g) is the mass of adsorbate per unit mass of the adsorbent, C_e (mg/L) is the equilibrium concentration, while the constants K_f (L/g) and 1/n represent adsorption capacity and adsorption intensity, respectively [19].

IV. Results and Discussion

A. *Results of Characterization of Activated Carbon*

Proximate analysis of the dried raw sugarcane bagasse (Table I) showed a fixed carbon concentration of 19.1%, which made it a suitable precursor for production of activated carbon [20]. Following calcination and activation, the volatile matter content reduced from 72.6 to 14.3%, while the fixed carbon, which is the main adsorption medium, increased from 19.1 to 69.7%. The SBAC had moisture content of 6.2%, which was indicative of good quality activated carbon [20].

TABLE I. PROXIMATE ANALYSIS OF THE SBAC

Parameter	Raw Dried Sugarcane Bagasse	SBAC
Moisture (%)	2.3	6.15
Volatiles (%)	72.6	14.3
Fixed carbon (%)	19.1	69.7
Ash (%)	6.0	9.85

Table II presents the results of the ultimate analysis of SBAC compared to the raw sugarcane bagasse. Calcination and activation increased the carbon content from 45.4 to 69.9%, which was attributed to release of the volatile matter. The result was comparable to the observations of carbon content of 68.6% in commercially available activated carbon derived from coconut shells [21].

International Journal of Engineering Research & Technology (IJERT)
ISSN: 2278-0181
Vol. 11 Issue 09, September 2022

TABLE II. ULTIMATE ANALYSIS (WT%) VALUES OF SUGARCANE BAGASSE AND ITS ACTIVATED CARBON

Parameter	Raw Sugarcane Bagasse	SBAC
Carbon (%)	45.4	69.9
Hydrogen (%)	7.7	3.5
Nitrogen (%)	1.1	2.7
Oxygen (%)[a]	45.8	23.9

[a] Concentration of oxygen obtained by the method of differences

The nitrogen adsorption-desorption isotherms were obtained by plotting the volume of nitrogen adsorbed per unit mass of SBAC against the relative pressure (p/po). The SBAC displayed Type I of International Union of Pure and Applied Chemistry (IUPAC) classification of adsorption isotherms with a convex curve whose platform was almost horizontal (Fig. 1). Type I isotherms occur where the pore size is not substantially larger than the molecular diameter of the sorbate molecules; consequently, the adsorption increases with relative pressure until it reaches saturation, at which point no further adsorption occurs. The results suggested that the nitrogen molecules are mainly adsorbed in the microporous structure with pore size 0 - 2 nm.

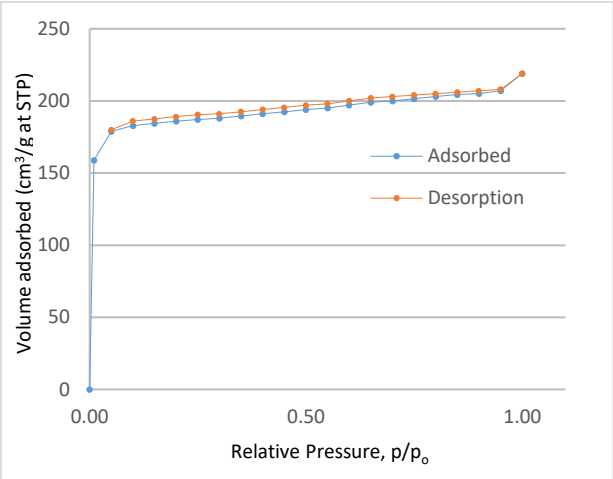

Fig. 1. SBAC Nitrogen Adsorption and Desorption Isotherms

Table III presents the Brunauer, Emmett and Teller (BET) surface area, total pore and micropores volume, and average pore diameter obtained from N_2 adsorption isotherms for raw ground sugarcane bagasse and SBAC. The SBAC showed two orders of magnitude increase in BET surface area and micropores volume over the raw ground sugarcane bagasse, an order of magnitude increase in total pore volume and an order of magnitude decrease in average pore diameter, which were attributed to the calcination and activation processes. For the SBAC, micropores accounted for about 84% of the pores volume; the remaining 16% of pores were likely to be mesopores. Significant surface area of 756.8 m^2/g was achieved, which was within the acceptable range of 500-1500 m^2/g for commercial activated carbon [13].

TABLE III. BET SURFACE AREA, TOTAL PORE VOLUME, MICROPORE VOLUME AND AVERAGE PORE DIAMETER OF RAW SUGARCANE BAGASSE AND SBAC

Sample	BET surface area (m2/g)	Total pore volume (cm^3/g)	Micropore volume (cm^3/g)	Average pore diameter (Å)
Raw Dried Sugarcane Bagasse	7.015	0.013	0.001	278.8
SABC	756.8	0.374	0.315	18.3

The Scanning Electron Microscope (SEM) images for SBAC (Fig. 2) revealed that the longitudinal texture and porosity of sugarcane bagasse were retained during the calcination and activation processes. However, holes, pits and some axial wedge fractures were observed. The pyloysis of the volatile matter from the bagasse leaves a porous carbonaceous structure. During activation, H_3PO_4 may have corroded unconverted biomass residue to form numerous micropores with large specific surface area.

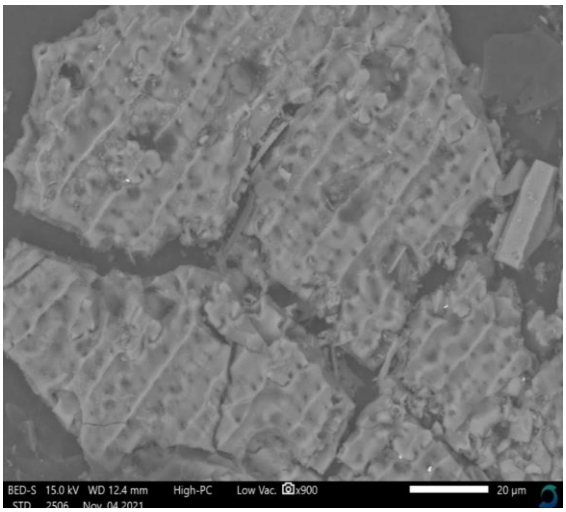

Fig. 2. SEM images of SBAC

Fig. 3 shows the Fourier Transform Infrared (FT-IR) spectra for the SBAC. At 3,362 cm^{-1}, the broad and flat band associated with the hydroxyl group can be attributed to the adsorbed water. The weak absorption peak at 1,912 cm^{-1} is probably due to the C=C stretching vibration. The band visible at 1,592 cm^{-1} corresponds to the stretching vibration of the C=O. The peak at 1190 cm^{-1} may be assigned to the stretching mode of hydrogen-bonded P=O, O–C stretching vibrations in P–O–C (aromatic) linkage, and to P=OOH [22]. The shoulder at 1100 cm^{-1} was ascribed to ionized linkage P–O– in acid phosphate esters, and to symmetrical vibration in a P–O–P chain [23]. The presence of the P-O- demonstrated that a reaction occurred between H_3PO_4 and the carbonised sugarcane bagasse. In addition, the FTIR spectrum of the activated carbon fibers has a weak absorption peak at 847.66 cm^{-1}, which is attributed to the bending vibration of the C–H bond in the high degree of substitution of the aromatic ring. The results indicated that the hydrogen content in the aromatic ring was enhanced by the activation. The introduction of phosphorus containing functional groups in the calcined sugarcane bagasse may play an important role in removal of fluoride from water.

International Journal of Engineering Research & Technology (IJERT)
ISSN: 2278-0181
Vol. 11 Issue 09, September 2022

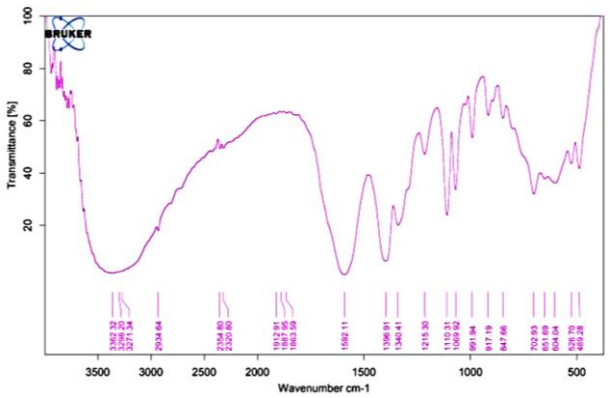

Fig. 3. FT-IR Spectra of SBAC

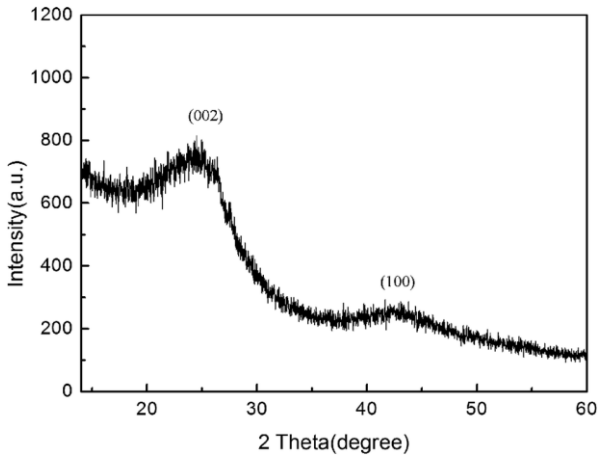

Fig. 4. X-ray diffraction of the SBAC

The XRD was used to determine the crystallinity of the SBAC. The activated carbon exhibited very broad X-ray diffraction peaks (Figure 4), which together with the absence of sharp peaks reveals a predominantly amorphous structure [24]. There were two broad diffraction peaks around 2θ = 24° and 43° in spectrum, corresponding to the diffraction of (0 0 2) and (1 0 0), respectively. The appearance of the peak at around 24° signified an increasing regularity of crystalline structure following calcination, which would result in a better layer alignment [25]. The result of XRD analysis was consistent with the SEM images, which revealed a morphology of carbonaceous material with numerous pores.

The SBAC had a bulk density of 0.53 g/cm^3, which was within the typical range of 0.35 to 1.2 g/m^3 for carbonaceous materials [26]. Generally, a moderate bulk density is desirable as a balance between the requirements for porosity and structural strength.

An activated carbon yield of 65.0% was observed, which indicated significant carbon content in the sugarcane bagasse feedstock. The yield is comparable to the 55.2 to 64.4% yield obtained in activation of coconut shell with lime and commercial potash [27].

B. Results of Fluoride Removal from Groundwater

Water samples collected from a borehole in Nakuru Town had a fluoride concentration of 6.7 mg/l, which exceeded the WHO guideline limit of 1.5 mg/l (Table IV). However, the pH was within the recommended range of 6.5 – 8.5.

TABLE IV. CHEMICAL AND PHYSICAL ANALYSIS OF GROUNDWATER WATER SAMPLE

Parameter	Value	WHO guideline value for drinking water
Fluoride (mg/L)	6.7	<1.5
pH	6.5	6.5-8.5

C. Results of Contact Time and Adsorbent Dosage Tests

The adsorbent dosage and contact time adsorption tests were conducted with an initial fluoride concentration of 7.0 mg/L at pH 6.5 for SBAC dosages 5 to 25 g in 250 ml of simulated fluoride water. The SBAC removed more than 50% of the initial fluoride concentration in the first 30 minutes for all the adsorbent dosages (Fig. 5). The rate of removal of fluoride reduced with time as the active sites decreased and also became less accessible. Larger adsorbent doses provided more active sites, which increased fluoride removal but at a lesser proportion. Achieving a residue fluoride concentration of within the WHO guideline value of less than 1.5 mg/L required a dose of 20 g /250 ml of water and a contact time of 5 h. Consequently, further adsorption tests applied the test conditions.

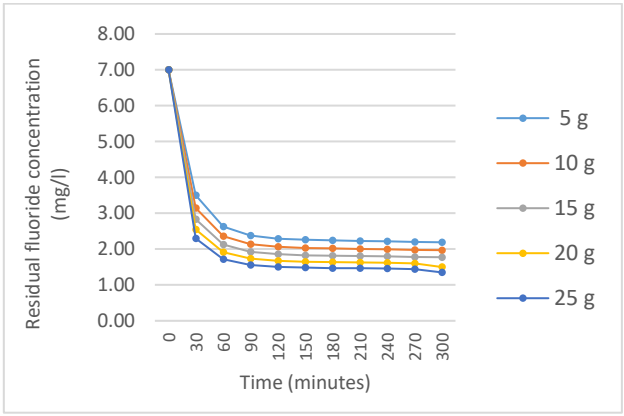

Fig. 5. Variation of residual fluoride concentrations for different adsorbent SBAC doses in 250 ml of simulated with time for initial fluoride concentration 7.0 mg/L and pH 6.5

D. Effect of pH on Fluoride Removal

The efficiency of fluoride removal was tested for pH 3 to 9. Fig. 6 shows fluoride removal reduced marginally from 87% at pH 3 to 86 % pH 5 and then significantly to 75% at pH 9.

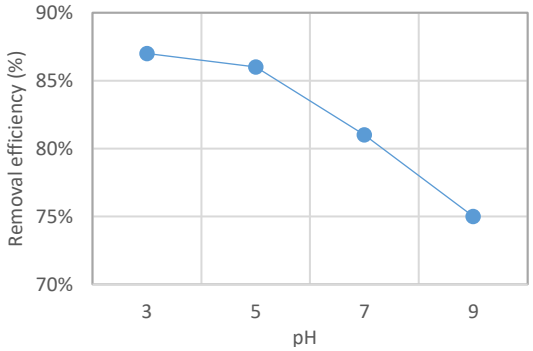

Fig. 6. Effect of pH on fluoride removal efficiency at 20 g SBAC per 250 ml dosage, contact time, 5 h and initial fluoride concentration 7.0 mg/L

International Journal of Engineering Research & Technology (IJERT)
ISSN: 2278-0181
Vol. 11 Issue 09, September 2022

In the acidic medium, the surface of the adsorbent is highly protonated; therefore, strong coulombic force of attraction between positively charged surface and negatively charged fluoride ion increases fluoride sorption to the SBAC. In alkaline medium, the repulsion between negatively charged surface (deprotonated) and fluoride ions lead to lesser fluoride adsorption.

E. Results of Initial Fluoride Concentration Tests

Tests for initial fluoride concentration were conducted at SBAC dosage of 20 g per 250 ml of fluoridated water. As shown in Fig. 7, the removal efficiency of the adsorbent decreased with increase in initial fluoride concentration from 86% at initial fluoride concentration of 5 mg/L to 78% for 25 mg/L. Higher removal efficiencies at lower initial fluoride concentrations were attributed to higher ratio of active surface area to total fluoride ions, leading to the utilization of the more accessible and energetically active sites on the adsorbent surface. On the other hand, increase in initial fluoride concentration may have resulted in insufficient surface area to accommodate the increased fluoride ions in solution and thereby decreased removal efficiency [28]. Additionally, for the SBAC, the previously observed large proportion of micropores could reduce the accessibility of some of the sites.

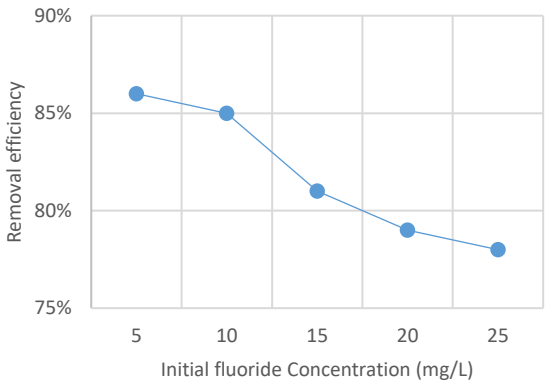

Fig. 7. Effect of initial fluoride concentration on removal efficiency at conditions: 20 g SBAC per 250 ml dosage, 5 h contact time, pH 3.

F. Results of Tests on Groundwater Samples

The efficiency of fluoride removal with SBAC was tested for groundwater samples from Nakuru Town with a fluoride concentration of 6.7 mg/L, at adsorbent dosage 20 g/250 ml and pH 3. Adsorption with SBAC reduced the fluoride concentration by 82.7% to 1.16 mg/L, which was within the WHO guideline value of 1.5 mg/L fluoride concentration. The removal was less than the 86% for simulated fluoride water, which was attributed to competition for active sites by CO^{-} existing anions such as PO_4^{3-}, Cl^{-}, SO_4^{2-}, Br^{-}, NO^{3-} and HCO^{3-}.

G. Adsorption isotherms

The Langmuir isotherm (Fig. 8) fitted the adsorption data poorly with an R^2 value of 0.717 as compared to Freundlich isotherm 0.990 (Fig. 9). The failure of the Langmuir isotherm to adequately describe the adsorption data suggests a lack of uniformity on the SBAC surface, which was consistent with the previous observations with the SEM. Nevertheless, the equilibrium parameter, R_L, was less than 1 (Table V) indicating favorable adsorption whereby a large amount of adsorption occurs at low absorbate concentrations [18]. Similarly, the Freundlich 1/n value of less than 1 (Table VI) suggests a diminishing tendency for sorption with increasing loading.

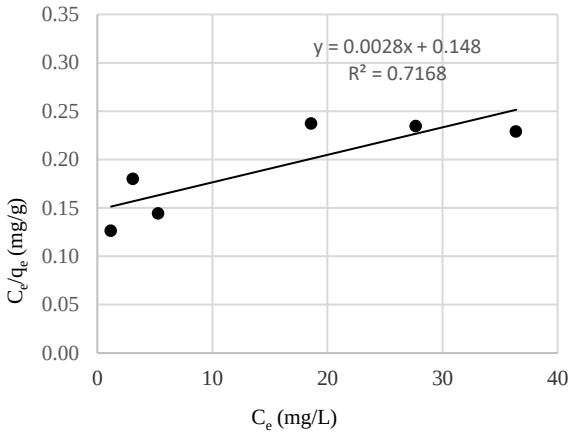

Fig. 8. Langmuir Isotherm for SBAC adsorption of Fluoride

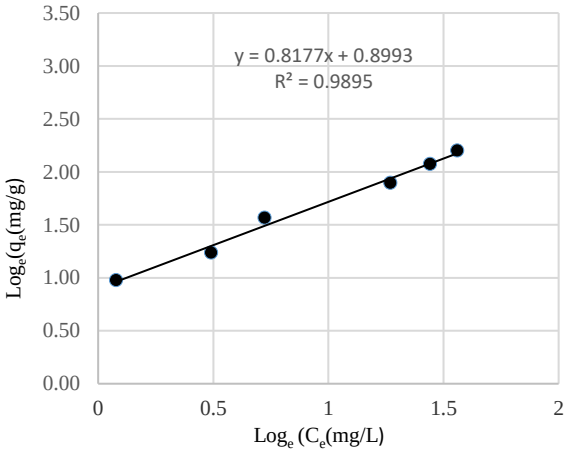

Fig. 9. Freundlich Isotherm for SBAC adsorption of Fluoride

TABLE V. LANGMUIR ADSORPTION ISOTHERM PARAMETERS AND CORRELATION COEFFICIENTS

Isotherm	**Langmuir**			
Parameter	b (L/g)	Q_{max} (mg/g)	R^2	R_L
Isotherm value	0.0189	357.1	0.7168	0.35-0.91

TABLE VI. FREUNDLICH ADSORPTION ISOTHERM PARAMETERS AND CORRELATION COEFFICIENTS

Isotherm	**Freundlich**		
Parameter	K_f	1/n	R^2
Isotherm value	2.456	0.8177	0.9895

V. CONCLUSIONS

This study characterized sugarcane bagasse derived activated carbon (SBAC) and evaluated its removal of fluoride from laboratory simulated fluoride water and groundwater with elevated concentrations of fluoride. Compared to the raw sugarcane bagasse, the SBAC had an enhanced fixed carbon

International Journal of Engineering Research & Technology (IJERT)
ISSN: 2278-0181
Vol. 11 Issue 09, September 2022

content of 69.7%. It also had a significant surface area of 756.8 m^2/g, which was within the acceptable range of 500-1500 m^2/g for commercial activated carbon. Micropores accounted for 84% of the total pore volume. FTIR spectrum revealed the presence of phosphorus containing functional groups including P–O-C and P–O–P; which could play a significant role in sorption of fluoride ions. The potential for the SBAC removal of fluoride from water was demonstrated by 86% removal from 7 mg/l fluoride simulated water with 20 g SBAC in 250 ml at 5 h contact time and pH 5, to achieve the permissible WHO limits of less than 1.5 mg/L. However, fluoride removal from groundwater was slightly less at 82.7%, which was attributed to competition for active sites by co-existing ions. The Langmuir isotherm described the adsorption data poorly with an R^2 value of 0.716 compared to Freundlinch 0.990 suggesting a lack of uniformity on the SBAC surface. Generally, the SBAC showed potential for use as an inexpensive biomass derived adsorbent for removal of fluoride from aqueous solution. However, further studies are recommended to establish recovery of the adsorbent.

CONFLICTS OF INTEREST

There is no conflict of interest to declare.

REFERENCES

[1] W. Nigussie, F. Zewge, and B.S. Chandravanshi, "Removal of excess fluoride from water using wasteresidue from alum manufacturing process," 2007.

[2] A. Rafique, M.A. Awan, A. Wasti, I.A. Qazi, and M. Arshad, "Removal of fluoride from drinking water using modified immobilized activated alumina," Journal of Chemistry, 2012, vol. 13.

[3] World Health Organization, Ed., Guidelines for drinking-water quality, 3rd ed. Geneva: World Health Organization, 2004.

[4] M. Suneetha, B.S. Sundar, and K. Ravindhranath, "Removal of fluoride from polluted waters using active carbon derived from barks of Vitex negundo plant," J Anal Sci Technol, vol. 6, no. 1, p. 15, 2015.

[5] E.W. Wambu, and G.K. Muthaka, "High fluoride water in the Gilgil Area of Nakuru County, Kenya," The International Society for Fluoride Research Inc, Research Report Fluoride, vol no. 1, pp. 37–41, 2011.

[6] M. Maina, E. Wambu, and J. K. Lusweti, "Analysis of Fluoride in Kales (Brassicca oleracea) and Tomatoes (Lycopersicum esculentum) from Nakuru County, Kenya," AER Journal, vol. 4, no. 1, pp. 35–42, 2020.

[7] J. Grimm, D. Bessarabov, and R. Sanderson, "Review of Electro-assisted methods for water purification," Institute for Polymer Science, University of Stellenbosch, Matieland 7602, P/Bag X1, Stellenbosch, South Africa, 1998.

[8] H. Demelash, A. Beyene, Z. Abebe, and A. Melese, "Fluoride concentration in ground water and prevalence of dental fluorosis in Ethiopian Rift Valley: systematic review and meta-analysis," BMC Public Health, vol. 19, 2019.

[9] S. Saidi, F. Boudrahem, I. Yahiaoui, and F. Aissani-Benissad, "Agar-agar impregnated on porous activated carbon as a new adsorbent for Pb(II) removal," Water Science and Technology, vol. 79, no. 7, pp. 1316–1326, 2019.

[10] R.H. Hesas, A. Arami-Niya, W.M.A.W. Daud, and J.N. Sahu, "Preparation of granular activated carbon from oil palm shell by microwave-induced chemical activation: Optimisation using surface response methodology," Chemical Engineering Research and Design, vol. 91, no. 12, pp. 2447–2456, 2013.

[11] R.W.S.W. Suraya, M.A.M. Razi, and H. Rafidah, "Overview of acid optimization in impregnation method for sugarcane bagasse activated carbon production," Advances in Environmental Biology, vol. 9, no, 12, pp. 1–14, 2015.

[12] V.K. Gupta and Suhas, "Application of low-cost adsorbents for dye removal – A review," Journal of Environmental Management, vol. 90, no. 8, pp. 2313–2342, 2009.

[13] A. R. Hidayu, N. F. Mohamad, S. Matali, and A. S. A. K. Sharifah, "Characterization of Activated Carbon Prepared from Oil Palm Empty Fruit Bunch Using BET and FT-IR Techniques," Procedia Engineering, vol. 68, pp. 379–384, 2013.

[14] S. Brunauer, P. H. Emmett, and E. Teller, "Adsorption of Gases in Multimolecular Layers," J. Am. Chem. Soc., vol. 60, no. 2, pp. 309–319, 1938.

[15] S.R. Popuri, Y. Vijaya, V.M. Boddu, and K. Abburi, "Adsorptive removal of copper and nickel ions from water using chitosan coated PVC beads," Bioresource Technology, vol. 100, no. 1, pp. 194–199, 2009.

[16] I.B. Solangi, S. Memon, and M.I. Bhanger, "Removal of fluoride from aqueous environment by modified amberlite resin," Journal of Hazardous Materials, vol. 171, no. 1–3, pp. 815–819, 2009.

[17] J. Fito, H. Said, S. Feleke, and A. Worku, "Fluoride removal from aqueous solution onto activated carbon of Catha edulis through the adsorption treatment technology," Environ Syst Res, vol. 8, no. 25, 2019.

[18] S. Chen, J. Zhang, C. Zhang, Q. Yue, Y. Li, and C. Li, "Equilibrium and kinetic studies of methyl orange and methyl violet adsorption on activated carbon derived from Phragmites australis," Desalination, vol. 252, no. 1–3, pp. 149–156.

[19] J.F. Nure, N.T. Shibeshi, S.L. Asfaw, W. Audenaert, and S.W.H. Van Hulle, "COD and colour removal from molasses spent wash using activated carbon produced from bagasse fly ash of Matahara Sugar Factory, Oromiya Region, Ethiopia," Water SA, vol. 43, no. 3, pp. 470–479, 2017.

[20] M. De, R. Azargohar, A.K. Dalai, and S. R. Shewchuk, "Mercury removal by bio-char based modified activated carbons," Fuel, vol. 103, pp. 570–578, 2013.

[21] W. Daud, "Comparison on pore development of activated carbon produced from palm shell and coconut shell," Bioresource Technology, vol. 93, no. 1, pp. 63–69, 2004.

[22] A.M. Puziy, O.I. Poddubnaya, A. Martínez-Alonso, F. Suárez-García, and J.M.D. Tascón, "Synthetic carbons activated with phosphoric acid," Carbon, vol. 40, no. 9, pp. 1493–1505, 2002.

[23] S. Bourbigot, M. Le Bras, R. Delobel, P. Bréant, and J. Trémillon, "Carbonization mechanisms resulting from intumescence-part II. association with an ethylene terpolymer and the ammonium polyphosphate-pentaerythritol fire retardant system," Carbon, vol. 33, no. 3, pp. 283–294, 1995.

[24] W.-H. Wang, Q. Wei, and H.Y. Bai, "Enhanced thermal stability and microhardness in Zr–Ti–Cu–Ni–Be bulk amorphous alloy by carbon addition," Appl. Phys. Lett., vol. 71, no. 1, pp. 58–60, 1997.

[25] K. Gedik and I. Imamoglu, "Removal of cadmium from aqueous solutions using clinoptilolite: Influence of pretreatment and regeneration," J. Hazardous Materials, vol. 155, no. 1–2, pp. 385–392, 2008.

[26] N. Jerome Sunday, "Quantitative Characterization of Activated Carbon from Cow, Donkey, Chicken and Horse Bones from Ezzangbo in Ebonyi State, Nigeria," AJAC, vol. 6, no. 5, p. 169, 2018.

[27] V. E. Efeovbokhan et al., "Preparation and characterization of activated carbon from plantain peel and coconut shell using biological activators," J. Phys.: Conf. Ser., vol. 1378, no. 3, p. 032035, 2019.

[28] T. Getachew, A. Hussen, and V. M. Rao, "Defluoridation of water by activated carbon prepared from banana (Musa paradisiaca) peel and coffee (Coffea arabica) husk," Int. J. Environ. Sci. Technol., vol. 12, no. 6, pp. 1857–1866, 2015.